Temperature Effects on Thermomechanical Properties of Elastomeric Stamps for Micro Transfer Printing Applications

C. Reyes[1,2], J. O. Thostenson[1], K. Oswalt[1], J. Roe1[1], D. Gomez[1]
1 - X-Celeprint Inc., Research Triangle Park, NC 27709
2 - Corresponding Author, creyes@x-celeprint.com

Introduction

Micro-transfer printing (MTP) enables mass-transfer of wafer-level chips having lateral dimensions ranging from 3 x 7 um to 650 x 650 um to a nonnative target wafer. This technology has been in used in industry for over a decade with a multitude of applications that are continuously expanding. [1] These applications include the micro transfer printing of micro pixel drivers for OLED displays, conventional micro LEDs for active and passive displays, solar concentrators for micro solar arrays, IIIV lasers and photonics. [4-10] This is accomplished using an elastomeric stamp with micro post that have been precisely defined using photolithography. MTP is highly parallel and is capable of transferring over 80,000 devices in a single MTP operation. [11] Transfer yields and placement accuracy, ±1.5µm 3σ, however, are dependent on the thermomechanical performance of the multilevel elastomer stamp. [12]

Chiplets to be transferred are first released using a chemical etching process, leaving them suspended and ready for picking. Small microstructures at the end of the stamp, referred to as posts, are placed in contact with the chiplets using a high precision print tool. The posts stick to the chiplets via van der Waals forces [13]. During the pick, the stamp moves vertically rapidly, breaking the tether connecting the device from the source substrate, **Fig 1a**. The stamp, with device attached to the post, is positioned over the target, aligned to a specific marker, then placed, **Fig 1b**. The stamp consists of a Polydimethylsiloxane (PDMS) elastomer mounted on a rigid glass substrate, **Fig 1c**. The MTP process has been studied and described in further detail in previous reports [11-14]

Given the high precision and accuracy needed to successfully MTP thousands of micron sized devices, knowing the behavior of the stamp under various temperatures is critical. These initial simulations show that temperature increases can deform the stamp enough to cause misalignment during the MTP process. Future work will include the simulation of various stamp and post designs to mitigate the effects of thermal expansion. This will give industries utilizing MTP a tool to design stamps capable of transferring more devices than previously possible with predictable placement accuracy.

In this work, we utilize the Structural Mechanics Module with Heat Transfer in Solids as well as Solid Mechanics to investigate heat distribution and thermal expansion. The simulation is based off the Thermal Expansion in a MEMS Device model from the Applications Library. In this study, an elastomeric stamp with a 2 x 2 array of micro posts is simulated to investigate heat distribution and thermal expansion. Volume expansion of the stamp and movement of the post are measured as these factors directly affect placement accuracy.

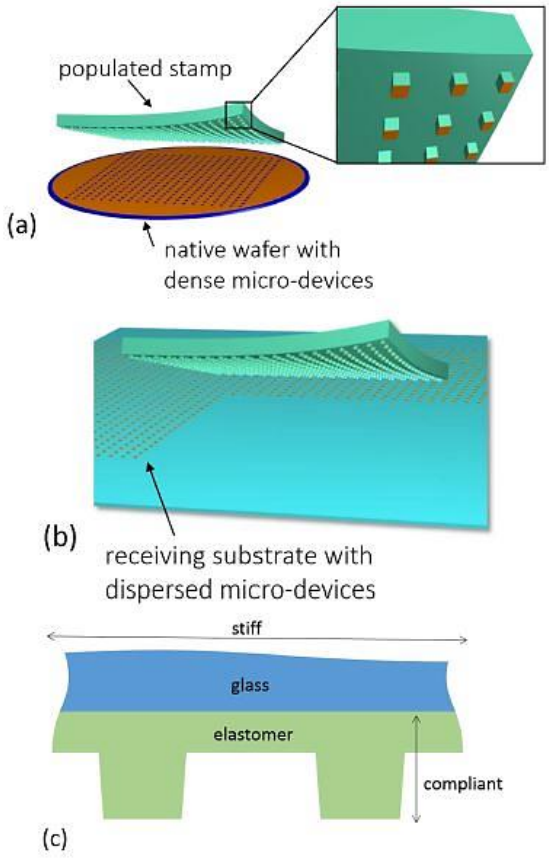

Figure 1. Cartoon of the micro transfer printing process. a) the stamp picks released devices from the source substrate then the stamp then transfers the devices to a non-native target wafer b). c) is a cross section schematic of the stamp. [image - ref 13]

Theory / Experimental Set-up

The model consists of two sets of physics: A thermal expansion with a convective heat source heating the stamp. The heat flux is applied at all boundaries except the base which is thermally insulated. All domains are subject to solid heat equations with the PDMS material properties providing all inputs. In practice, the stamp is mounted on a glass substrate which may affect heat transfer because of the differences in thermal conductivities, but we are only

concerned with the behavior of the PDMS stamp at specific temperature, i.e. equilibrium temperatures. Thus, the method of heat transfer to the stamp is of less concern than the physical implications due to thermal expansion.
For solid mechanics analysis, the physical forces are balanced with a volume load caused by thermal expansions and PDMS stamp is fixed at the base of the largest cube. Fixing the base of the stamp in the model reflects the physical application of the stamp mounted on a rigid glass that is noncompliant. The effect of possible thermal expansion for the elastomer stamp is investigated.

The stamp is designed after an actual test stamp used at X-Celeprint consisting of a base, intermediate layer and microposts, **Fig 2**. In the simulation, the base, intermediate layer, and posts comprise 3 separate domains joined by a union. The posts are cubes placed in a 2x2 array with a given x-y pitch. In practice, the pitch and array are determined by the size of the chiplet to be transferred. What we wish to determine is how the stamp thermally expands and what is the deviation in the x-y and z directions.

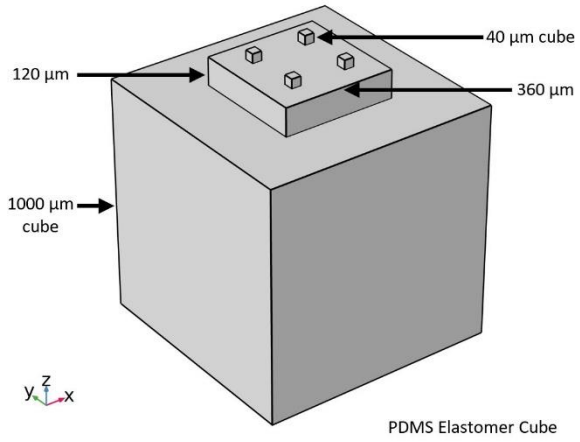

Figure 2. 3D Model of PDMS stamp with a 4 post array.

Simulation Methods

This model used in the report is similar in design to the Application titled *Thermal Expansion in a MEMS Devices.* This model leverages the use of COMSOL Multiphysics Thermal Expansion, Structural Mechanics and Thermal Heat Transfer in Solids modules.

The conditions for the Solid Mechanics module are as follows: The base boundary is set to *Fixed* while all other boundaries are set to *Free*. All three domains, base, intermediate and posts are *Linear Elastic.* This reflects the application conditions with the base of the stamp fixed to the rigid glass substrate. The thermal expansion of the glass substrate is negligible in the temperature range considered in the simulations. The equations that govern the linear elastic physics are shown in **figure 3** below.

$$\rho\frac{\partial^2\mathbf{u}}{\partial t^2} = \nabla\cdot S + \mathbf{F}_V$$

$$S = S_{ad} + \underline{\mathbf{C}:\epsilon_{el}}, \quad \epsilon_{el} = \epsilon - \epsilon_{inel}$$

$$\epsilon_{inel} = \epsilon_0 + \epsilon_{ext} + \epsilon_{th} + \epsilon_{hs} + \epsilon_{pl} + \epsilon_{cr} + \epsilon_{vp}$$

$$S_{ad} = S_0 + S_{ext} + S_q$$

$$\epsilon = \frac{1}{2}\left[(\nabla\mathbf{u})^T + \nabla\mathbf{u}\right]$$

Figure 3. Equations for linear elastic materials within the solid mechanics module.

Here, ρ is the density of the PDMS, S is the Cauchy stress tensor, F_v is the force volume, ε is strain, ε_{el} and ε_{inel} are elastic and inelastic strain respectively. **u** is the displacement vector, S_{ad} **,** S_{ext} and **,** S_q are the deviatoric stress, external stress tensor and extra stress due to visco dampening respectively. The initial displacement and force vectors are set to 0 in x,y and z directions.

For the Heat Transfer in Solids module, the base boundary is set to *Insulating*, while the remaining boundaries are set to *Convective Heat Flux.* Again, it is worth noting that are several methods of applying heat in this application. For simplicity, convective heat flux gave us the heat range desired with the least amount of computational time. All three domains are subject to *Solid Heat Transfer.* The equations governing the heat transfer are shown in **figure 4** below.

$$-\mathbf{n}\cdot\mathbf{q} = \underline{q_0}$$

$$q_0 = h(T_{ext} - T)$$

Figure 4. Equations for Convective Heat Flux in materials within the Heat Transfer module.

Here, **n** is the dimensionless normal vector to the surface with heat flux, q is conductive heat flux, q_o is the inward heat flux, *h* is the heat transfer coefficient (1 W/m^2). T and Text are the initial and external temperatures, 293.15K and 350.15K, respectively.

The physical properties for PDMS were selected from the materials library and are summarized in **table 1** in the appendix.

Simulation Results & Discussion

We begin by examining the thermal behavior of the PDMS stamp. The stamp heats from room temp, 20 C, to a max temp of 26.7 C, **Fig 5.** The heating is linear as expected and the stamp appears to heat uniformly. The base of the stamp is ~0.2 C cooler than the post, **Fig 5.** This is due to the thermally insulated base condition but does reflect the application configuration where the stamp is mounted on glass that has a thermal conductivity 4-10x higher than the PDMS.

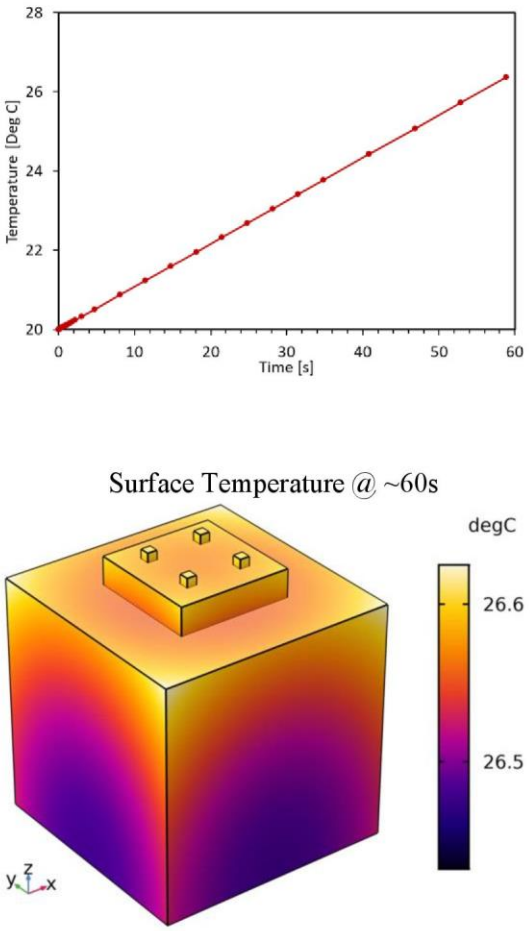

Figure 5. Top, temperature vs time for the average surface temperature of the stamp. Bottom, 3D surface plot of the average surface temperature at the end of the simulation.

These temperature ranges are higher than what would be experiences in real world printing applications (20-22C), but we wanted to examine the effects at extreme conditions.

Next, we want to investigate the geometric effect the heat has on the volume expansion. For this, we employed the volume displacement arrow plot to visualize the outward expansion. The arrows are plotted in an 8 x 8 x8 array and are proportional in length. They do show an outward expansion with the largest expansion at the corners and edge of the base and outward movement increases as you deviate from the fixed substrate. This is also what is seen in practical applications. To quantify the movement, we placed probe points on edges and on the posts to measure the volume displacement as well as the distance the posts move from each other. **Figure 7** below plots the results of the volume displacement measurements.

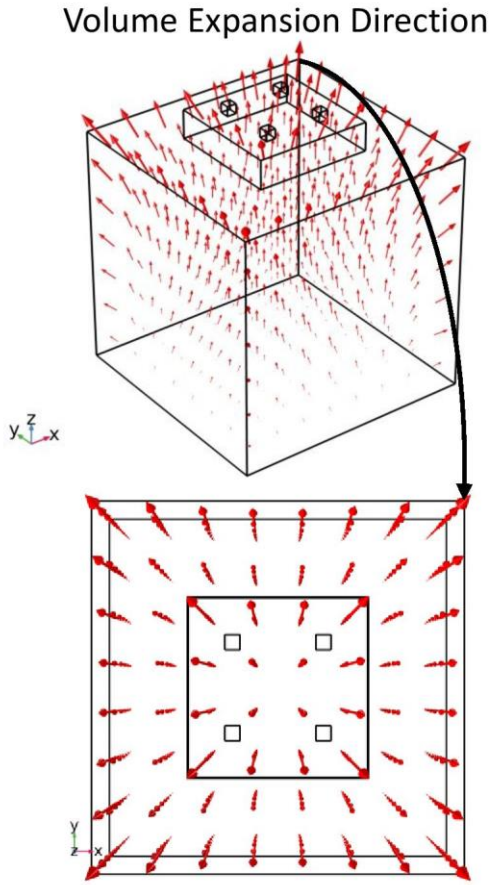

Figure 6. Volume arrow displacement of the cube during simulation.

The effects of this movement can be seen in the von mises stresses (**Fig A1)** with the stresses concentrated at the base were it is constrained to the glass. There is no noticble stresses between the base-intermediate layer and internediate layer-post. This is due to the elastic nature of PDMS and the *Free* and *Linear Elastic* conditions in the simulation. The final volume displacement (**Fig A1)** shows the volume displacemetn increases from the fixed based to the top of the posts as expected.

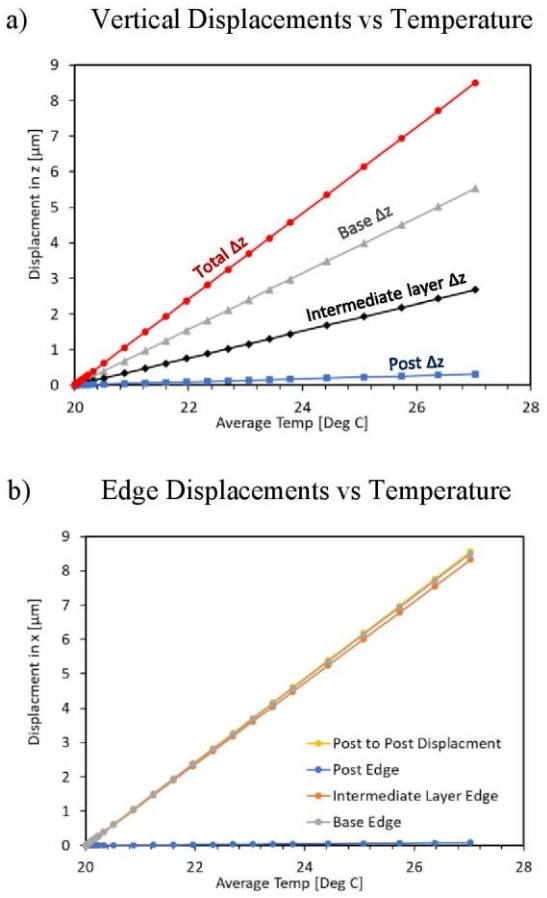

Figure 7. a) Vertical height displacements of the base, intermediate layer and post. b) edge displacements of the base, intermediate layer, posts and post to post.

These results show that the expansion of the stamp is small , < 1 µm, within typical operating conditions. Beyond 21C, tjermal is signifigant and the movement of the posts is beyond the alignment accuracty of the printer, **±1.5µm 3σ.** The height of the entire stamp moves significantly in the z direction, 8.142 µm. This can be detrimental to picking and printing as picking requires precise z direction control to avoid pressing the chiplet into is native substrate, causing it to stick to the subrate, rendering it unpickable.

The post to post deviation is extremely important in picking and printing of densely populated source and target substrates. The results reveal that within typical operating conditions, the post can deviate up to 1.1 µm from their original positions. This is exacerbated at elevated temperatures causing the posts to move 8.573 µm. This would render the printer in operable as this is would cause the stamp to pick unwanted chiplets and the placement would be impossible to place in an array.

Conclusions

In this work, we utilize the Structural Mechanics Module with Heat Transfer in Solids as well as Solid Mechanics to investigate heat distribution and thermal expansion. We found that 1 degree C of thermal expansion above room temp is enough to displace the posts used for picking chiplets 1-1.5 µm, which is at the placement accuracy of the microtransfer printing process. At elevated temperatures, thermal expansion can cause the posts to deviate as much as 8 µm from their original array positions as well as move significantly in the z directions. This can be catastrophic when picking and placing small, densely packed chiplets and would be impossible to place them precisely onto a substrate.

The results of these simulations are to be compared and validated with the stamp of the same geometry. Future work should involve the simulation of a larger array, 100 x100, as well as investigate geometries that mitigate thermal expansions. It is shown that accurate monitoring and control of the printing temperature is needed to ensure accurate and precise microtransfer printing operations.

References

1. E. Menard, K. J. Lee, D. Y. Khang, R. G. Nuzzo, J. A. Rogers, *Appl. Phys. Lett.* 84, 5398 (2004)
2. M.A. Meitl, Z.-T. Zhu, V. Kumar, K.J. Lee, X. Feng, Y.Y.Huang, I. Adesida, R.G. Nuzzo, and J.A. Rogers, "Transfer Printing by Kinetic Control of Adhesion to an Elastomeric Stamp," *Nature Materials* 5, 33-38 (2006).
3. J. Yoon, S. Lee, D. Kang, M. Meitl, C. Bower, J. Rogers, *Adv. Opt. Mat.*, 3, 1313 (2015)
4. A. Carlson , A. M. Bowen , Y. G. Huang , R. G. Nuzzo , J. A. Rogers, *Adv. Mater., 24,* 5284 (2012)
5. C.A. Bower, E. Menard, S. Bonafede, J.W. Hamer, R.S. Cok, "Transfer-printed microscale integrated circuits for high performance display backplanes," *IEEE Transactions on Components, Packaging and Manufacturing* 1 (12), 1916-1922 (2011)
6. M. Meitl et al. Passive Matrix Displays with Transfer-Printed Microscale Inorganic LEDs. *Proceedings of Society for Information Display International Symposium*, v. 47, no. 1, 743-746 (2016)
7. E. Radauscher et al., "Miniaturized LEDs for flat-panel displays", *SPIE Proceedings*, v. 10124 (2017)
8. K. Ghosal amd M. Meitl, *Compound Semiconductor*, 5, 34 (2014)
9. J. Justice, C. A. Bower, M. Meitl, M. B. Mooney, M. A. Gubbins, B. Corbett. 9, 2012, *Nature Photonics*, Vol. 6, pp. 612-616.
10. B. Corbett, C. Bower, A. Fecioru , M. Mooney , M. Gubbins ,J. Justice, *Semicond. Sci. Tech.*, 28, 094001 (2013)
11. Gomez, D., Ghosal, K., Moore, T., Meitl, M. A., Bonafede, S., Prevatte, C., ... & Bower, C. A. (2017, May). Scalability and yield in elastomer stamp micro-transfer-printing. In 2017 IEEE 67th Electronic Components and Technology Conference (ECTC) (pp. 1779-1785). IEEE.
12. C.A. Bower, M.A. Meitl, S. Bonafede, D. Gomez, A. Fecioru and D. Kneeburg, "Heterogeneous integration of microscale compound semiconductor devices by micro-transfer printing, *IEEE Proceedings of Electronic Components and Technology Conference*, 963-967 (2015).
13. Gomez, D., Ghosal, K., Meitl, M. A. *et al.*, "Process Capability and Elastomer Stamp Lifetime in Micro Transfer Printing," *66th Electronic Components and Technology Conference (ECTC)*, 680-687 (2016).
14. B. Furman, E. Menard, A. Gray, M. Meitl, S. Bonafede, D. Kneeburg, K. Ghosal, R. Bukovnik, W. Wagner, J. Gabriel, S. Seel, S. Burroughs, *IEEE PVSC Proceedings*, 475 (2010)
15. C. Prevatte *et al.*, "Pressure-Activated Electrical Interconnection During Micro-Transfer-Printing", *66th Electronic Components and Technology Conference (ECTC)*, 1209-1215 (2016).

Appendix

Table 1: Material Properties

Property	Variable	Value	Unit	Property Group
Coefficient of thermal expansion	alpha_iso ; alphaii = alpha_iso, alphaij = 0	9e-4[1/K]	1/K	Basic
Heat capacity at constant pressure	Cp	1460[J/(kg*K)]	J/(kg·K)	Basic
Density	rho	970[kg/m^3]	kg/m³	Basic
Thermal conductivity	k_iso ; kii = k_iso, kij = 0	0.16[W/(m*K)]	W/(m·K)	Basic
Young's modulus	E	750[kPa]	Pa	Young's modulus and Poisson's ratio
Poisson's ratio	nu	0.49	1	Young's modulus and Poisson's ratio
Relative permittivity	epsilonr_iso ; epsilonrii = epsilonr_iso, epsilonrij = 0	2.75	1	Basic

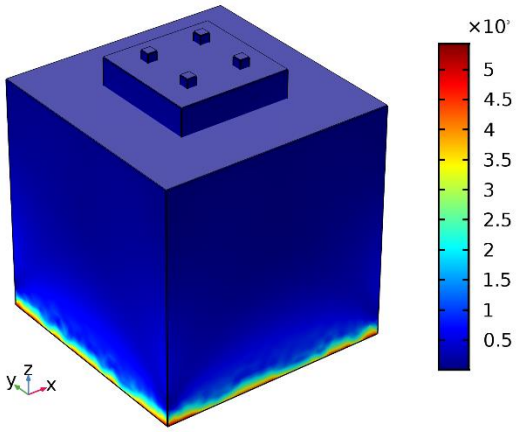

Figure A1. Von mises stress at the end of the simulation. Units are N/m^2.

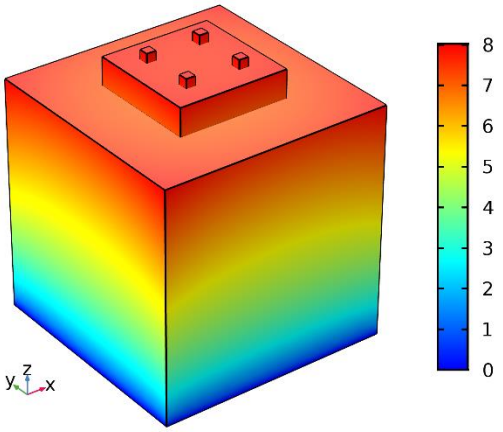

Figure A2. Average volume displacement at end of simulation. Units are in µm.